J Mater Sci (2024) 59:11468–11479

Materials for life sciences

Impedimetric monitoring of microRNA-200c-3p using hydroxyapatite nanoparticles modified pencil graphite electrodes

Gulsah Congur[1,*] and Arzum Erdem[2]

[1] Department of Pharmacy, Vocational School of Health Services, Bilecik Seyh Edebali University, 11100 Bilecik, Turkey
[2] Analytical Chemistry Department, Faculty of Pharmacy, Ege University, 35100 Bornova, İzmir, Turkey

Received: 26 December 2023
Accepted: 28 May 2024
Published online: 6 June 2024

ABSTRACT

It is important to monitor miRNA-200c-3p as it can potentially serve as an important biomarker for respiratory diseases including COVID-19 and cancer. Despite the importance of microRNA monitoring, there are few previous studies for miRNA-200c-3p monitoring, and the application of hydroxyapatite nanoparticles (HaNP) in miRNA biosensors is quite limited. This study aims to fill this gap by utilizing the advantageous properties of HaNPs to develop a powerful strategy to detect microRNA-200c-3p. First, HaNPs were modified on the surface of pencil graphite electrodes (PGEs). Subsequently, hybridization between a phosphate-labeled miRNA-200c-3p-specific DNA probe and its complementary RNA target was carried out in the solution phase. The DNA-RNA hybrid forms were immobilized on the surface of the HaNP-PGEs and the impedimetric measurements were performed. The changes at the charge transfer resistance value (R_{ct}) were evaluated in terms of the hybridization and optimization of the experimental conditions. The detection limits (DLs) were calculated as 0.12 µg/mL (16.19 nM) in phosphate buffer solution (PBS, pH 7.40) and 0.31 µg/mL (41.82 nM) in synthetic plasma. The selectivity of the developed biosensor was tested against miRNA-200c-5p and miRNA-141-3p. The results promise a significant improvement in public health in terms of a leap forward in the early diagnosis of many serious diseases.

Introduction

The field of research involving diagnosis and monitoring of miRNAs has gained popularity and importance over the years, as miRNAs are valuable biomarkers for the detection of vital diseases, including diabetes, cardiovascular diseases, cancer and neurological disorders [1–6]. Moreover, their existence in biological fluids opens a new perspective for researchers to develop non-invasive detection platforms for diagnosis

Handling Editor: Annela M. Seddon.

Address correspondence to E-mail: gulsah.congur@bilecik.edu.tr

https://doi.org/10.1007/s10853-024-09832-w

of the said vital diseases. Although mounting reports have been published for monitoring of miRNAs [7–9], there is still a great need for the application of nanomaterials in this field due to their unique properties. On the other hand, electrochemical biosensor systems incorporating nanotechnology have evolved from prototypes to lab-on-a chip systems [10–20], and as a result, a large group of researchers has focused on the development of electrochemical biosensors for the detection of miRNAs.

It has been reported that miRNA-200c-3p is associated with the regulation of angiotensin-converting enzyme 2 (ACE2), which is a receptor in the renin–angiotensin system [21]. Downregulation of ACE2 is associated with acute lung injury (ALI) and acute respiratory distress syndrome (ARDS) induced by different types of viruses. Liu et al. [21] reported that miRNA-200c-3p was upregulated by H5N1 virus infection, and elevated levels of miRNA-200c-3p were detected in the plasma samples of patients with severe pneumonia. In another study [22], upregulation of miRNA-200c-3p was found in angiotensin II (Ang II)-induced renal artery endothelial injury. The changes in miRNA-200c-3p levels are also associated with various cancers such as prostate cancer [23], papillary thyroid cancer [24], and endometrial cancer [25].

Hydroxyapatite ($Ca_{10}(PO_4)_6(OH)_2$, HAP) is a bioceramic naturally found in the structure of bone tissue [26, 27]. The HAP structure is defined as the most durable material that remains stable in liquids, in humid environments and at neutral or alkaline pH [28]. The nanoscale form of HAP (HaNP) provides a large surface area and enables the creation of durable biocompatible surfaces. HAP and HaNP have been used in various fields, including biosensors [29–41], due to their superior properties.

Electrochemical impedance spectroscopy (EIS) is a versatile method for understanding the interfacial reactions on the electrode surface by measuring the charge transfer resistance (R_{ct}) produced in the presence of a redox solution. Based on this principle, the modification of a biomaterial/nanomaterial or the biochemical reactions occurred between a bioreceptor and a target molecule can be specifically monitored using EIS technique [42]. Impedimetric biosensors are capable of the sensitive and selective recognition of different analytes such as proteins [43], drugs [44], nucleic acids [45], etc. Therefore, impedimetric biosensors are reliable prototypes of the commercial miniaturized monitoring tools. Although there are numerous advantageous properties of impedimetric biosensors as well as most of the electrochemical biosensors, the impedance measurements are quite complex compared to other electrochemical techniques, making this technique more labor intensive.

Herein, HaNP modified disposable pencil graphite electrodes (HaNP-PGEs) were developed for the electrochemical detection of miRNA-200c-3p as the first time in the literature. Electrochemical impedance spectroscopy (EIS) technique which enables fabrication of sensitive and selective biorecognition platforms [42–45], was used for the optimization of each experimental step and the detection of miRNA-200c-3p. The fabrication of the HaNP-PGEs was elucidated using both electrochemical and microscopic techniques, and the repeatability of the HaNP-PGEs was investigated under optimum conditions. After the optimization of experimental conditions for electrochemical miRNA-200c-3p detection, the selectivity and applicability of the HaNP-PGE-based impedimetric biosensor platform in synthetic plasma were studied. The detailed discussion about the results and future prospects are given in further sections.

Experimental evaluation

Apparatus

All electrochemical analyzes were carried out by IVIUM Compactstat.e (IVIUM Release 4.951 software package, Holland) in a three-electrode system as explained in our previous study [41].

Chemicals

The HaNP solution containing nanoparticles (< 200 nm, detailed information is available at https://www.sigmaaldrich.com/TR/en/product/aldrich/702153), and other chemicals such as $K_3[Fe(CN)_6]$, $K_4[Fe(CN)_6]$ and KCl used for the preparation of the redox solutions, and K_2HPO_4, KH_2PO_4 and NaCl used for the preparation of 50 mM phosphate buffer solution containing 20.00 mM NaCl (PBS, pH 7.40) were purchased from Sigma-Aldrich (Germany). All chemicals were of analytical grade. The synthetic bovine plasma was also purchased from Sigma-Aldrich (Germany) (detailed information is available at https://

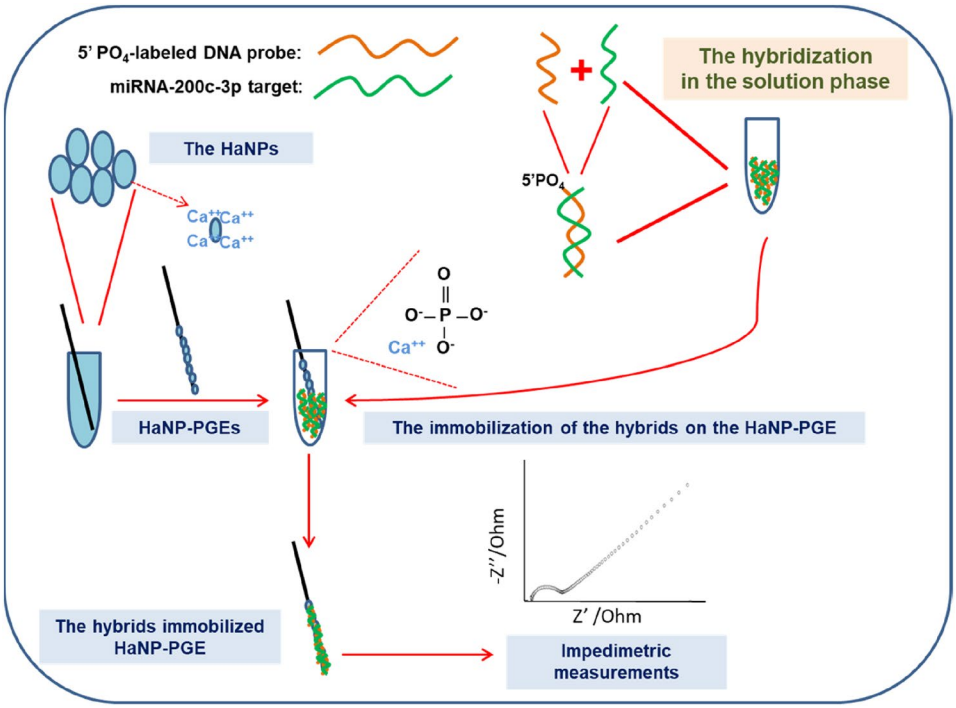

Scheme 1 The experimental procedure of the development of HaNP-PGE based impedimetric biosensor for the detection of miRNA-200c-3p.

www.sigmaaldrich.com/TR/en/product/sigma/p4639). The miRNA-200c-3p specific DNA probe and the RNA target were purchased from TIBMOLBIOL (Berlin, Germany). The oligonucleotide sequences are listed below:

miRNA-200c-3p specific DNA probe (phosphate labelled, 23 base-length):

5′-PO_4-TCC ATC ATT ACC CGG CAG TAT TA-3′

miRNA-200c-3p target RNA (23 base-length):

5′-UAA UAC UGC CGG GUA AUG AUG GA-3′

miRNA-200c-5p (22 base-length):

5′-CGU CUU ACC CAG CAG UGU UUG G-3′

miRNA-141-3p (22 base-length):

5′-UAA CAC UGU CUG GUA AAG AUG G-3′

Stock solutions of the oligonucleotides were prepared as 500.00 µg/mL in Tris EDTA buffer solution (10.00 mM Tris-HCl, 1 mM EDTA, pH 8.00), and stored frozen. The diluted solutions of the oligonucleotides were prepared in PBS, (pH 7.40).

Procedure

The procedure of the development of the HaNP-PGEs, the nucleic acid hybridization, and the EIS measurements was summarized in Scheme 1.

Preparation of the HaNP-PGEs

The stock concentration of HaNP solution was 10^5 µg/mL, and the diluted HaNP solutions of 10.00–40.00 µg/mL were prepared in PBS (pH 7.40). PGEs were dipped into 100 µL HaNP solution for 15 min [41]. Then, the electrodes were washed in PBS (pH 7.40) for 5 s.

The nucleic acid hybridization of miRNA-200c-3p specific DNA probe and its RNA target, and the sample immobilization at the surface of HaNP-PGEs

Nucleic acid hybridization was performed in the solution phase similar to our previous study [41]. In brief, the nucleic acid hybridization between phosphate-labeled DNA probe at the 5′ end and the target miRNA sequence was firstly performed. Then, the hybrid forms were immobilized on the HaNP-PGE surface due to the covalent bonds between the calcium groups of HaNP and the phosphate group of the hybrid form originating 5′ end of DNA probe [41]. miRNA-200c-3p DNA probe: RNA target (1:1) was prepared in PBS (pH 7.40) as 40 µL, and the samples were located in a shaker at 400 rpm. For the optimization of DNA probe concentration, the mixture of 0.002–0.05 µg/mL DNA probe: 2.00 µg/

mL RNA target was used, and the hybridization was performed for 15 min. For optimization of nucleic acid hybridization time, the mixture of 0.01 µg/mL DNA probe: 2.00 µg/mL RNA target was used, and the hybridization was performed for 15–90 min. For miRNA target concentration optimization, the hybridization was performed for 60 min in the presence of 0.01 µg/mL DNA probe: 1.00–8.00 µg/mL miRNA-200c-3p mixture.

After sample preparation, 20 µg/mL HaNP modified PGEs were transferred into the samples, and immobilization of the samples was carried out for 60 min by passive adsorption [41]. For the control experiments, DNA probe samples were prepared and treated as if the hybridization had been performed. Then, these samples were immobilized at the surface of HaNP-PGEs as explained.

Electrochemical measurements

Cyclic voltammetry (CV) measurements CV measurements were performed in 2.00 mM $K_3[Fe(CN)_6]$/$K_4[Fe(CN)_6]$ (1:1) prepared in 0.10 M KCl. The potential range was from − 0.50 to + 1.00 V, and the scan rate was 50.00 mV.

Electrochemical impedance spectroscopy (EIS) measurements EIS measurements were carried out in 2.50 mM $K_3[Fe(CN)_6]$/$K_4[Fe(CN)_6]$ (1:1) prepared in 0.10 M KCl. During the measurements, an open circuit potential as + 0.23 V (vs. Ag/AgCl/3M KCl) was applied to the electrochemical cell. The frequency was in the range of 10^5–10^{-1} Hz, and the sinusoidal signal was 10.00 mV. The Nyquist diagrams were fitted with the equivalent circuit shown in each figure. The parameters of the circuit are as follows: $\mathbf{R_S}$ is the solution resistance, **Q** is the constant phase element which refers to the space charge capacitance at the electrode–electrolyte interface, $\mathbf{R_{ct}}$ is the charge transfer resistance that occurs at the electrode–electrolyte interface. The constant phase element, **W** is the Warburg impedance due to mass transfer to the electrode surface.

Results and discussion

The microscopic characterization of the HaNP modification on the PGE surface was performed (Fig. 1). The layered graphite surface of PGE was successfully coated with 20.00 µg/mL HaNP after the modification (Fig. 1B), and this coated surface was clearly seen at each magnitude compared to the unmodified PGE (Fig. 1A). The EDX spectra and elemental concentrations of PGE and HaNP-PGE are shown in Fig. S1 and Table S1, respectively. The weight percent (wt%) and atomic percent (at%) values of O, Ca and P atoms increased sharply after HaNP modification on PGE, while the values of C atom decreased sharply (Table S1). These microscopic results indicate that

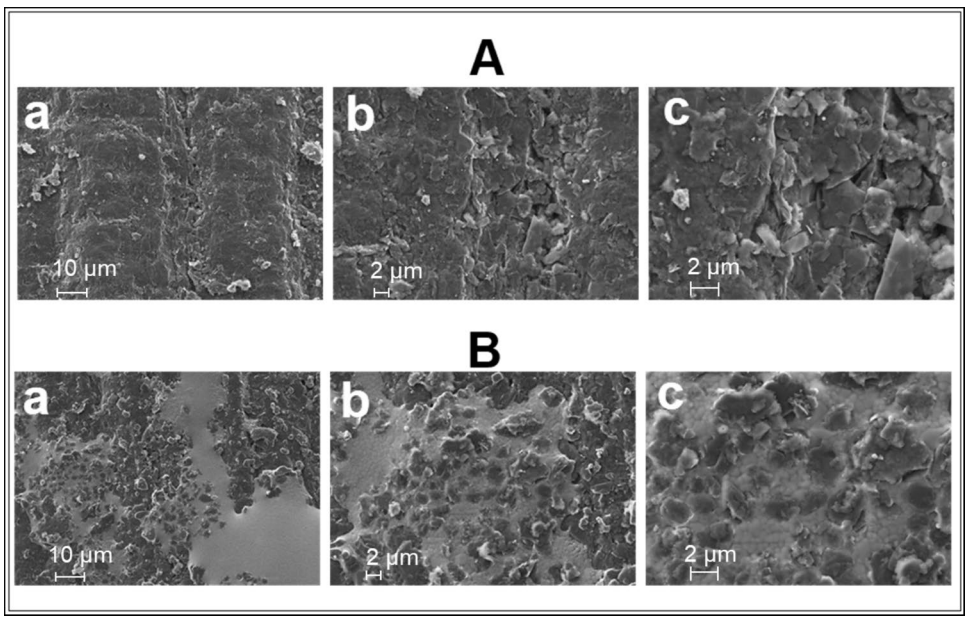

Figure 1 SEM images of PGE (**A**), 20 µg/mL HaNP modified PGE (**B**). The resolutions are 2000x (**a**), 5000x (**b**) and 10000x (**c**) and the acceleration voltage was 5.00 kV. All measurements were performed at Bilecik Seyh Edebali University Research and Application Center.

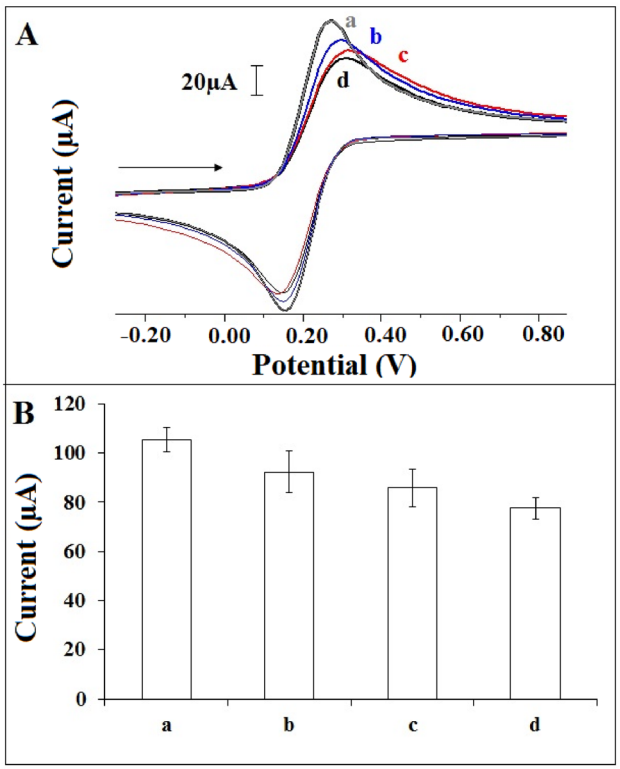

Figure 2 The cyclic voltammograms (**A**) the and the histograms (**B**) representing the average I_a values of PGEs (**a**), 20.00 μg/mL HaNP modified PGEs (**b**), DNA probe (**c**) or the hybrid form obtained after the hybridization of DNA probe: miRNA-200c-3p (1:1) (**d**) immobilized HaNP-PGEs (n = 3). The experimental conditions are: DNA probe concentration: 0.01 μg/mL, miRNA-200c-3p target miRNA concentration: 3.00 μg/mL, hybridization time: 60 min.

HaNP was successfully modified on the surface of PGE.

Electrochemical characterizations of the unmodified and 20.00 μg/mL HaNP modified PGEs, as well as the 0.01 μg/mL miRNA-200c-3p specific DNA probe immobilized or the hybrid form obtained after the hybridization of 0.01 μg/mL miRNA-200c-3p specific DNA probe:3.00 μg/mL miRNA-200c-3p target immobilized HaNP-PGE were investigated using the CV technique (Fig. 2). The average I_a value of the PGEs was measured to be 105.49 ± 4.84 μA (RSD% = 4.59%, n = 3) (Fig. 2B-a). After HaNP modification, the average I_a value decreased (Fig. 2B-b), which was the expected result due to the negative structure of HaNP [41]. After immobilization of the DNA probe, the average I_a value also decreased (Fig. 2B-c), which was due to the introduction of the negatively structured DNA oligonucleotide on the surface of the HaNP-PGE. The average I_a value after immobilization of the DNA probe was calculated to be 85.81 ± 7.79 μA (RSD% = 9.09%, n = 3). The behavior of I_a obtained after nucleic acid hybridization (Fig. 2B-d) was the same as when the DNA probe was immobilized on HaNP-PGE. The decrease in the average I_a value was the expected result as the negativity of the electrode increased after the nucleic acid hybridization of the negatively structured DNA probe and RNA target. After nucleic acid hybridization, the average I_a value of 77.54 ± 4.21 μA (RSD% = 5.44%, n = 3) was obtained. The calculated surface area (A_{eff}) values for each group using the Eq. S1 were represented in Table S2, and it was seen that the A_{eff} values decreased after each modification/immobilization step which was the similiar behavior with the I_a value. These results are consistent with the results reported in previous studies [46, 47].

The optimization studies were started with the determination of optimum HaNP concentration for modification of the disposable PGEs (Fig. S2). After HaNP modification of PGE, the R_{ct} value increased as a result of the repulsive interactions between the negative HaNPs and the PGE surface [41]. The highest average R_{ct} value was obtained after 20 μg/mL HaNP modification on the PGE surface (Fig. S2-A, B-c), and the average R_{ct} value was recorded to be 221.04 ± 28.46 Ohm, (RSD% = 12.88%, n = 3). This concentration level of HaNP was chosen as optimum for the modification. The reproducibility of the HaNP-PGEs were investigated by preparing six different groups of the HaNP-PGEs (Fig. S3). The average R_{ct} values obtained by the HaNP-PGEs prepared in six different groups were 212.00 ± 11.53 Ohm, 212.00 ± 2.58 Ohm, 211.25 ± 21.72 Ohm, 216.00 ± 15.64 Ohm, 217.67 ± 21.39 Ohm, 229.00 ± 18.03 Ohm (n = 3) with the RSD% values as 5.44%, 8.67%, 10.28%, 7.24%, 9.82%, 7.87%, respectively. These results indicate that the HaNP-PGEs showed reproducible behavior.

The studies were continued by the optimization of miRNA 200c-3p specific DNA probe concentration (Fig. S4). The nucleic acid hybridization between 0.002–0.05 μg/mL DNA probe and 2.00 μg/mL RNA target was conducted for 15 min, and the average R_{ct} values were recorded before and after the nucleic acid hybridization for each concentration level. The R_{ct} value increased after the immobilization of DNA probe or the hybrid forms which was in consistency with the results obtained by the CV technique [46, 47]. The most reproducible and the highest R_{ct} value after the nucleic acid hybridization was obtained in

the presence of 0.01 µg/mL DNA probe (Fig. S4E-III). The average R_{ct} values obtained before and after the hybrization in the presence of 0.01 µg/mL DNA probe and 2.00 µg/mL RNA target were found to be 438.40 ± 108.71 Ohm and 542.33 ± 42.53 Ohm (n = 3) with the RSD% values as 24.80% and 7.84%, respectively.

In the next step of our study, the nucleic acid hybridization time was optimized in the presence of 0.01 µg/mL DNA probe and 2.00 µg/mL RNA target by applying 15–90 min hybridization time (Fig. 3). The average R_{ct} values obtained before and after the hybridization were compared in terms of the increase ratios. The highest increase ratio as 57.66% and the most reproducible responses were obtained by 60 min hybridization (Fig. 3-II-D). The average R_{ct} values obtained before and after the hybridization were recorded to be 382.00 ± 58.35 Ohm and 602.25 ± 52.80 Ohm with the RSD% values as 15.27% and 8.77% (n = 3), respectively.

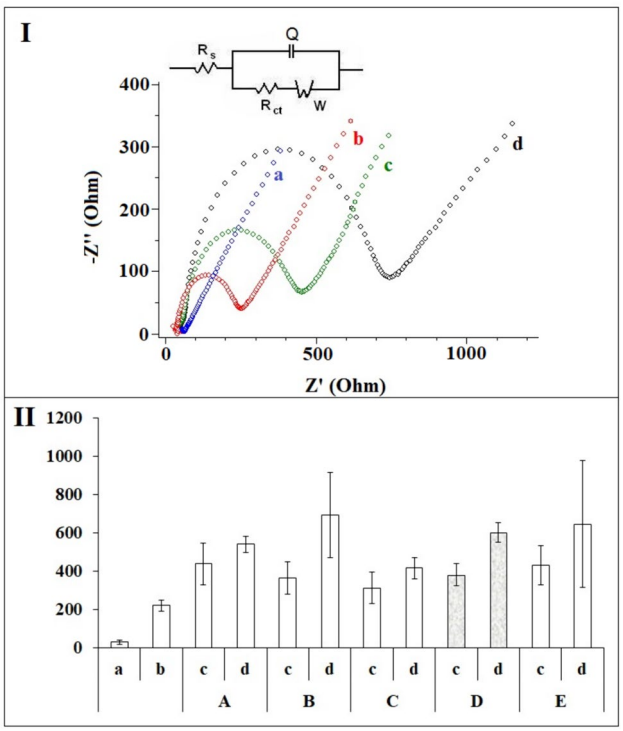

Figure 3 The Nyquist diagrams (**I**) of PGE (**a**), HaNP-PGE (**b**), before (**c**) and after (**d**) the hybridization of 0.01 µg/mL miRNA-200c-3p DNA probe: 2.00 µg/mL target miRNA 200c-3p (1:1) for 60 min. The average R_{ct} values (n = 3) (**II**) of PGE (**a**), HaNP-PGE (**b**), before (**c**) and after (**d**) the hybridization of 0.01 µg/mL miRNA-200c-3p DNA probe: 2.00 µg/mL target miRNA 200c-3p (1:1) for 15 min (**A**), 30 min (**B**), 45 min (**C**), 60 min (**D**) and 90 min (**E**).

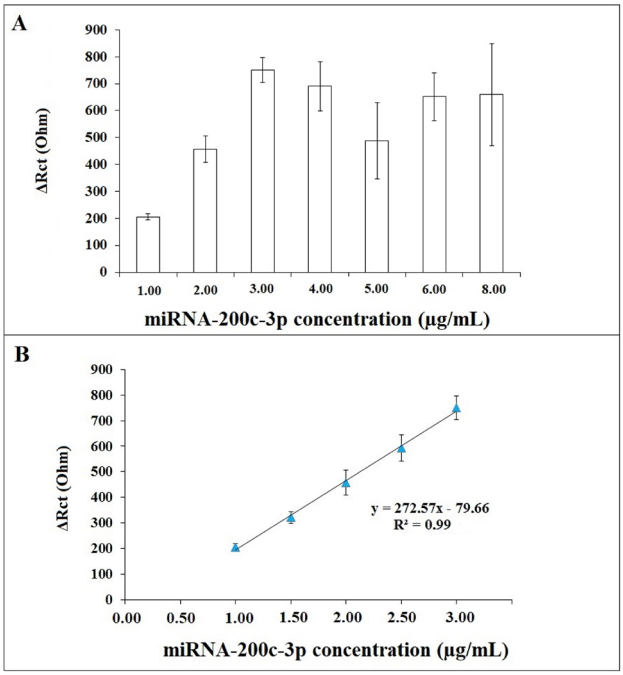

Figure 4 The average ΔR_{ct} values (**A**) obtained after the hybridization of 0.01 µg/mL miRNA-200c-3p DNA probe and 1.00–8.00 µg/mL miRNA-200c-3p target. Line graph (**B**) based on the average ΔR_{ct} values obtained after the hybridization of 0.01 µg/mL miRNA-200c-3p DNA probe and 1.00–3.00 miRNA-200c-3p target (n = 3).

60 min Hybridization time was determined as optimum hybridization time, and the studies continued by searching the effect of miRNA concentration upon the impedimetric biosensor response (Fig. 4). For this purpose, the nucleic acid hybridization was conducted in the presence of 0.01 µg/mL DNA probe and 1.00–8.00 µg/mL RNA target for 60 min. In this part of the study, ΔR_{ct} values were calculated based on the Eq. 1, and the highest ΔR_{ct} value was obtained in the presence of 3.00 µg/mL RNA target as 751.00 ± 46.72 Ohm (RSD% = 6.22%, (n = 3)). This concentration level was chosen as optimum. The detection limit (DL) was calculated to be 0.12 µg/mL (16.19 nM) based on the calibration graph (Fig. 4-B) obtained in the concentration range of 1.00–3.00 µg/mL RNA target with the equation y = 272.57x − 79.66 and R^2 = 0.99 [48].

$$\Delta R_{ct} = R_{ct2} - R_{ct1} \quad (1)$$

R_{ct2} = The R_{ct} value obtained DNA probe/hybrid form immobilized HaNP-PGE.R_{ct1} = The R_{ct} value obtained by HaNP-PGE.

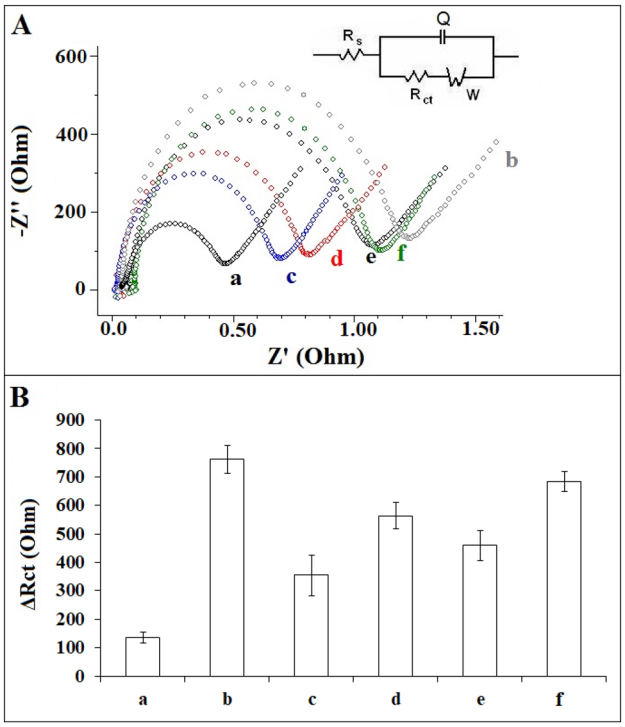

Figure 5 The Nyquist diagrams (**A**) and the histograms representing the average ΔR_{ct} (**B**) values (n = 3) of 0.01 µg/mL miRNA-200c-3p specific DNA probe immobilized HaNP-PGE (**a**), the hybrid forms obtained by the hybridization of 0.01 µg/mL miRNA-200c-3p specific DNA probe: 3.00 µg/mL miRNA-200c-3p target (**b**)/miRNA-200c-5p (**c**)/miRNA-141-3p (**d**) (1:1) immobilized HaNP-PGE, the hybrid forms obtained by the hybridization of 0.01 µg/mL miRNA-200c-3p specific DNA probe: 3.00 µg/mL miRNA-200c-3p target + miRNA-200c-5p (**e**)/miRNA-200c-3p target + miRNA-141-3p (**f**) immobilized HaNP-PGE.

The selectivity of the impedimetric biosensor was tested against miRNA-200c-5p that is in the same cluster with miRNA-200c-3p and miRNA-141-3p that is from the second cluster of miRNA-200c [21] (Fig. 5) under optimum conditions. The average ΔR_{ct} values were represented in Table S3. The highest average ΔR_{ct} value was obtained in the presence of miRNA-200c-3p RNA target that indicated the impedimetric biosensor had a selective behaviour against other selected miRNAs. The ΔR_{ct} decreased after the hybridization of miRNA-200c-3p DNA probe and the mixture of target miRNA + other miRNAs. However, the biosensor responses were still higher than the ones obtained in the presence of miRNA-200c-5p or miRNA-141-3p. It is concluded that HaNP-PGE based impedimetric biosensor represented selective behaviour.

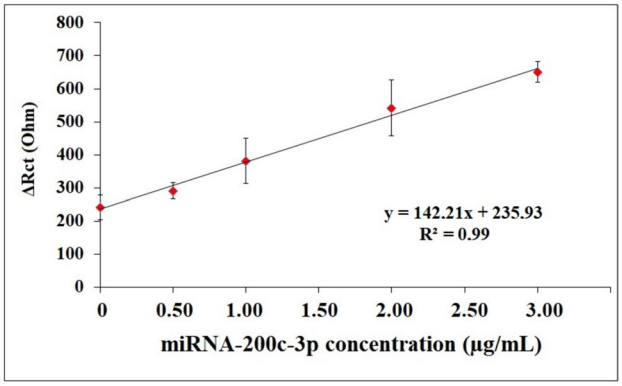

Figure 6 Line graph based on the average ΔR_{ct} values (n = 3) obtained by the hybridization of 0.01 µg/mL miRNA-200c-3p specific DNA probe: 0.00–3.00 µg/mL miRNA-200c-3p target in 1:5000 plasma: PBS (pH 7.40) for 60 min.

The application of the biosensor in synthetic plasma sample was tested to prove whether the developed biosensor platform could work in a complex media. First, the hybridization was performed in plasma or diluted plasma samples and ΔR_{ct} values were calculated according to Eq. 1 (Fig. S5). The ΔR_{ct} values obtained after the hybridization in in the presence of 1:1000 (Fig. S5-D) and 1:5000 (Fig. S5-E) diluted plasma samples were close to the one obtained in PBS (pH 7.40) (Fig. 4A). The average ΔR_{ct} values (n = 3) obtained after the hybridization in 1:1000 or 1:5000 diluted plasma samples were as 503.50 ± 195.90 (RSD% = 38.90%) Ohm and 650.50 ± 31.82 (%RSD = 4.89%) Ohm, respectively. More reproducible impedimetric response was obtained in 1:5000 diluted plasma sample. 1:5000 dilution ratio was selected for plasma dilution, and the effect of miRNA-200c-3p RNA target concentration upon the biosensor response was investigated. Figure 6 represents the calibration graph obtained based on the average ΔR_{ct} values (n = 3) in the presence of 0.00–3.00 µg/mL miRNA-200c-3p in 1:5000 diluted plasma. The DL was found to be 0.31 µg/mL (41.82 nM) [48] with the equation and R^2 values as y = 142.21x + 235.93 and 0.99, respectively.

Numerous reports were introduced in the literature for the electrochemical detection of miRNAs, and some of the recently published studies were represented in Table 1 [13–15, 49–57]. miRNA-21-5p was monitored [15] due to its role in the autophagy and its capability as a new treatment option for neurological diseases in combination with exosomes [58]. The monitoring of miRNA-21 was studied by many groups since it is a

Table 1 Some of the recently reported studies for electrochemical detection of miRNAs

miRNA type	Electrode	Nanomaterial/ biomaterial	Fabrication time	Electrochemical method	DL	Media	Refs
miRNA-19b	mSPGE	AuNP	~15 h	Amperometry	10.00 pM	Serum	[13]
miRNA-124	SPGE	–	~7 h	SWV	0.28 aM	Serum	[14]
miRNA 21-5p	SPE	AuNP	~3 h	EIS	4.31 aM	Serum	[15]
miRNA-21, miRNA-141	SPE	–	~20 h	CV, chronoamperometry	–	Urine	[49]
miRNA-21	GCE	Ti_3C_2@Bi_2O_3 nanocomposite and AuNP	~90 h	DPV	0.16 fM	Serum	[50]
	AuE	AuNP	~18 h	Chronocoulometry	10 aM	Serum	[51]
	GCE	MN, HaNP	~20 h	SWV	0.27 aM	Serum and cell lysate	[52]
miRNA-141	GCE	AuNP	~8 h 30 min	SWV	3.23 aM	Serum	[53]
miRNA-let-7a	GCE	Nafion/MWNTs and Ag@CPDs	~5 days and 11 h	LSV	30.00 fM	Serum	[54]
miRNA-155	AuE	g-C_3N_4@AgNPs	~48 h	AdsSV	50.00 and 100.00 fM (LOQ)	Serum	[55]
miRNA-126	AuE	CoNi-MOF	~88 h	EIS	0.14 fM	C6 cells	[56]
miRNA-200c-3p	PGE	HSA-AuNPs	~14 h 15 min	EIS	1.13 fM	Serum	[57]
	PGE	HaNP	~2 h 15 min	EIS	0.12 µg/mL (16.19 nM) in PBS (pH 7.40) and 0.31 µg/mL (41.82 nM) in plasma	Plasma	This work

Electrodes: *SPE* Screen printed carbon electrode, *GCE* Glassy carbon electrode, *mSPGE* Multi-array screen-printed gold electrode, *AuE* Gold electrode, *SPGE* Screen prointed gold electrode, *PGE* Pencil graphite electrode. Nanomaterials/biomaterials: *AuNP* Gold nanoparticles. *$Ti3C_2$@Bi_2O_3* Accordion-like Bi_2O_3-decorated titanium aluminum carbide nanocomposites, *Ag@CPDs* Ag@carbonized polymer dots, *MWNTs* Multiwalled carbon nanotubes, *g-C_3N_4@AgNPs* Graphitic carbon nitride @ silver nanoparticles, *CoNi-MOF* Bimetallic CoNi-based metal–organic framework, *MN* Magnetic nanoparticle, *HaNP* Hydroxyapatite nanoparticle, *HSA-AuNPs* Human serum albumin conjugated AuNPs, Electrochemical methods: *EIS* Electrochemical impedance spectroscopy, *CV* Cyclic voltammetry, *SWV* Square wave voltammetry, *DPV* Differential pulse voltammetry, *AdsSV* Adsorptive stripping voltammetry, Others: *LOQ* limit of quantification, *C6 cells* rat glioma cells

biomarker for not only several cancer types [49–52] but also cardiovascular diseases [51], and found in urine [49], and serum [50–52]. miRNA-141 is also associated with colorectal cancer and prostate cancer [49, 53]. Other miRNAs given in Table 1 are related with several cancer types [13, 54–57] and retinal degeneration [14]. The applicability of the biosensor systems was studied in mostly serum [13, 15, 50–55, 57], but cell lysates [52, 56] and urine [49] was also analyzed for the miRNA detection. The use of nanomaterials/biomaterials and their nanocomposites was preferable [15, 50–56] to increase the sensitivity and robustness of the biosensors. Although high sensitive and selective behaviour for a biosensor system is crucial, being practical and time-saving are also crucial properties to obtain feasible prototypes that lead to develop novel commercial diagnostics in future. At this point, most of the biosensor platforms in Table 1 required to spend significant amount of time from hours to days, and to use intensive chemical agents for the construction of the biosensor platforms. On the other hand, disposable platforms are preferable to eliminate implementing the experimental procedures for reusability. Therefore, single use electrodes such as SPE-based [13–15,

49] and PGE-based [57] electrochemical biosensors are one step further in comparison to other biosensors which have been fabricated by AuE [51, 55, 56] and GCE [50, 52–54].

Nanoparticles and their nanocomposites have been widely applied for the development of electrochemical miRNA biosensors. However, there is a limited number of reports in the literature for the use of the HaNPs in an electrochemical miRNA biosensor design [52, 59]. Liu et al. [52] reported a GCE based voltammetric biosensor for miRNA-21 detection. They combined magnetic nanoparticles (MNs) with duplex-specific nuclease (DSN) enzyme as the first time in the literature. They synthesized carboxylated MNs and immobilized biotinylated capture probe of miRNA-21 (CP) via crosslinking agents on the surface of MNs. They modified HaNPs with streptavidin (SA) using polyethylenimine (PEI) and glutaraldehyde, and mixed these modified HaNPs to obtain MNs/CP/HaNP probe. For hybridization, they followed the reaction between DSN, miRNA-21 and MNs/CP/HaNP probe by mixing and heating this mixture at 50 °C for 50 min, and removed the unbinding of CP and HaNP by magnetic separation. Finally, they incubated miRNA-21, the solution and sodium molybdate ($Na_2MoO_4{\cdot}2H_2O$) at the GCE surface to perform the reaction between the phosphate group of HaNP and $Na_2MoO_4{\cdot}2H_2O$. They implemented square wave voltammetry (SWV) technique to measure redox-active molybdophosphate as the biosensor response. Although this biosensor platform showed high sensitivity and specificity by showing a selective behaviour, the preparation steps are exhausting, and require to use several complex chemicals that result in the increase at the fabrication costs of the biosensor.

Although its importance in the different biological pathways was enlighted in several researches, the limited number of report for the detection of miRNA-200c-3p was found in the literature. In one of these studies, Kuang et al. [60] performed the detection of miRNA-200c-3p by developing a spectroscopic method in combination with duplex-specific nuclease (DSN)-mediated amplification strategy. Briefly, they synthesized a new DNA-peptide probe using a substrate peptide included reporter peptide and biotinylated miRNA-200c-3p specific DNA probe. After the specific hybridization of this DNA probe and miRNA-200c-3p RNA target, the double-stranded form was cleavaged in the presence of DSN, and the reporter peptide was released for the quantitative detection of miRNA-200c-3p using liquid chromatography − tandem mass spectrometry (LC–MS/MS) technique. The DL was found to be 1 fM in this study, and the selectivity of the developed detection method was shown against miRNA-200b, miRNA-141, miRNA-21, and single base mismatched miRNA sequences. This novel detection strategy possessed a sensitive and selective behavior for the detection of the target miRNA. However, it required to use several enzymes, and its implementation required to spend long times. In another aspect, LC–MS/MS technique does not enable to miniaturize the overall detection strategy that limits the field applications.

A PGE based impedimetric detection platform was reported in the literature for the monitoring of miRNA-200c-3p which is the only study in the literature for the electrochemical detection of miRNA-200c-3p [57]. In that report, gold nanoparticles conjugated with human serum albumin (HSA-AuNPs) was synthesized to take advantage of the AuNPs that have good electrical properties and of HSA that is the most abundant protein in plasma and has numerous binding sites. The research group modified the surface of PGE using these nanoparticles, and then immobilized thiolated DNA probe that was specific for miRNA-200c-3p. They performed the nucleic acid hybridization on the surface of the HSA-AuNPs/PGE, and evaluated the ΔR_{ct} value calculated by the differences between the R_{ct} values obtained after the hybridization and before the hybridization. Although there is a similarity between that report and this study, long experimental time was required to develop the said biosensor. The modification was carried out in 250 µL samples that is quite higher than the sample volumes used in this report (100 µL for HaNP modification and 40 µL for the hybridization). The selectivity studies were carried out in the presence of miRNA-410 and miRNA-192 in that report while the selectivity of the HaNP-PGE based impedimetric biosensor was tested herein in the presence of miRNA-200c-5p and miRNA-141-3p that are in the same cluster with miRNA-200c-3p and is from the second cluster of miRNA-200c [21]. Last but not least, this report is the first study in the literature that aimed to the integration of HaNP-PGEs for the electrochemical miRNA detection.

Conclusion

Herein, a novel electrochemical biosensor platform for the miRNA detection is reported. The main purpose of this research is to apply HaNPs for potential electrochemical detection of a model miRNA, specifically, miRNA-200c-3p as the first time in the literature. miRNA-200c-3p was chosen due to its role in COVID-19 infection progression and other diseases. A sensitive and selective monitoring of miRNA-200c-3p was achieved under optimum conditions, and the applicability of the HaNP-PGEs for miRNA detection was tested in synthetic plasma. This study represents the fabrication of a prototype for future hand-held devices for the monitoring of miRNAs. This study will pave the way for other researchers who aim to demonstrate the potential application of HaNPs in biosensors fabrication, specifically miRNA biosensors. This technique will facilitate and accelerate diagnostic and therapeutic protocols that will improve human health.

Acknowledgements

This study was supported by Bilecik Seyh Edebali University Scientific Research Project Coordination (Project no. 2021-01.BŞEÜ.12-02).

Author contributions

GC: Conceptualization, project administration, funding acquisition, ınvestigation, methodology, experimental design, carrying out experimental measurements, visualization, writing—original draft, writing—review and editing. AE: Conceptualization, investigation, supervision, methodology, experimental design, visualization, writing—original draft, writing—review and editing.

Funding

Open access funding provided by the Scientific and Technological Research Council of Türkiye (TÜBİTAK).

Declarations

Conflict of interests The authors declare no competing interests.

Supplementary Information The online version contains supplementary material available at https://doi.org/10.1007/s10853-024-09832-w.

References

[1] Yue J (2011) miRNA and vascular cell movement. Adv Drug Deliv Rev 63(8):616–622
[2] Wang SS et al (2018) A meta-analysis of dysregulated miRNAs in coronary heart disease. Life Sci 215:170–181
[3] Chakraborty C et al (2020) The interplay among miRNAs, major cytokines, and cancer-related inflammation. Mol Ther Nucleic Acids 20:606–620
[4] Ghafouri-Fard S, Shoorei H, Taheri M (2020) miRNA profile in ovarian cancer. Exp Mol Pathol 113:104381
[5] Juźwik CA et al (2019) microRNA dysregulation in neurodegenerative diseases: a systematic review. Prog Neurobiol 182:101664
[6] Feng J, Xing W, Xie L (2016) Regulatory roles of microRNAs in diabetes. Int J Mol Sci 17:1729
[7] Meng T et al (2020) An enzyme-free electrochemical biosensor based on target-catalytic hairpin assembly and Pd@UiO-66 for the ultrasensitive detection of microRNA-21. Anal Chim Acta 1138:59–68

[8] Meng T et al (2020) Pd nanoparticles-DNA layered nanoreticulation biosensor based on target catalytic hairpin assembly for ultrasensitive and selective biosensing of microRNA-21. Sens Actuators B Chem 323:128621
[9] Ling L et al (2022) Addressing the clinical feasibility of adopting circulating miRNA for breast cancer detection, monitoring and management with artificial intelligence and machine learning platforms. Int J Mol Sci 23:15382
[10] Cimmino W et al (2023) Design of a printed electrochemical strip towards miRNA-21 detection in urine samples: optimization of the experimental procedures for real sample application. Anal Bioanal Chem 415:4511–4520
[11] Caratelli V et al (2022) Liquid biopsy beyond cancer: a miRNA detection in serum with electrochemical chip for non-invasive coeliac disease diagnosis. Adv NanoBiomed Res 2:2200015
[12] Zouari M et al (2020) Femtomolar direct voltammetric determination of circulating miRNAs in sera of cancer patients using an enzymeless biosensor. Anal Chim Acta 1104:188–198
[13] Xu Y et al (2022) Tetrahedral DNA framework based CRISPR electrochemical biosensor for amplification-free miRNA detection. Biosens Bioelectron 217:114671
[14] Dastidar MG et al (2023) A simple yet highly sensitive and selective aptasensor architecture for rapid and portable miRNA detection. Chem Eng J 454:140186
[15] Serrano VM et al (2022) Carbon electrodes with gold nanoparticles for the electrochemical detection of miRNA 21–5p. Chemosensors 10:189
[16] Erdem A, Congur G, Eksin E (2013) Multi channel screen printed array of electrodes for enzyme-linked voltammetric detection of microRNAs. Sens Actuators B Chem 188:1089–1095
[17] Eksin E et al (2021) Paper-based electrode assemble for impedimetric detection of miRNA. Talanta 225:122043
[18] Yarali E et al (2022) Impedimetric detection of miRNA biomarkers using paper-based electrodes modified with bulk crystals or nanosheets of molybdenum disulfide. Talanta 241:123233
[19] Khodadoust A et al (2023) High-performance strategy for the construction of electrochemical biosensor for simultaneous detection of miRNA-141 and miRNA-21 as lung cancer biomarkers. Talanta 252:123854
[20] Khodadoust A et al (2022) A ratiometric electrochemical DNA-biosensor for detection of miR-141. Microchim Acta 189:213
[21] Liu Q et al (2017) miRNA-200c-3p is crucial in acute respiratory distress syndrome. Cell Discov 3:17021
[22] Liu Y et al (2020) MicroRNA-200c-3p inhibits proliferation and migration of renal artery endothelial cells by directly targeting ZEB2. Exp Cell Res 387(2):111778
[23] Zhang J et al (2019) MicroRNA-200c-3p/ZEB2 loop plays a crucial role in the tumor progression of prostate carcinoma. Ann Transl Med 7:141
[24] Feng YL et al (2022) MicroRNA-200c-3p negatively regulates ATP2A2 and promotes the progression of papillary thyroid carcinoma. Biochem Genet 60:1676–1694
[25] Srivastava A et al (2018) A non-invasive liquid biopsy screening of urine-derived exosomes for miRNAs as biomarkers in endometrial cancer patients. AAPS J 20:1–11
[26] Ibrahim M et al (2020) Hydroxyapatite, a multifunctional material for air, water and soil pollution control: a review. J Hazard Mater 3835:121139
[27] Fihri A et al (2017) Hydroxyapatite: a review of syntheses, structure and applications in heterogeneous catalysis. Coord Chem Rev 347:48–76
[28] Kaviya M et al (2021) Synthesis and characterization of nano-hydroxyapatite/graphene oxide composite materials for medical implant coating applications. Mater Today Proc 36:204–207
[29] Chen G, Zhitomirsky I, Ghosh R (2019) Fast, low-pressure chromatographic separation of proteins using hydroxyapatite nanoparticles. Talanta 199:472–477
[30] Avila JD et al (2020) Additively manufactured Ti6Al4V-Si-hydroxyapatite composites for articulating surfaces of load-bearing implants. Addit Manuf 34:101241
[31] Ma Y et al (2020) Preparation of hydroxyapatite with high surface area and dispersity templated on calcium carbonate in dipeptide hydrogels. Colloids Surf A 596:124740
[32] Sughanthy SAP, Ansari MNM, Atiqah A (2020) Dynamic mechanical analysis of polyethylene terephthalate/hydroxyapatite biocomposites for tissue engineering applications. J Mater Res Technol 2:2350–2356
[33] Shen G, Cai C, Yang J (2011) Fabrication of an electrochemical immunosensor based on a gold–hydroxyapatite nanocomposite–chitosan film. Electrochim Acta 56:8272–8277
[34] Wang S et al (2010) Hydroxyapatite nanoarray-based cyanide biosensor. Anal Biochem 398:191–197
[35] Kanchana P, Sekar C (2015) Development of electrochemical folic acid sensor based on hydroxyapatite nanoparticles. Spectrochim Acta Part A Mol Biomol Spectrosc 137:58–65
[36] Kanchana P, Navaneethan M, Sekar C (2017) Fabrication of Ce doped hydroxyapatite nanoparticles based non-enzymatic electrochemical sensor for the simultaneous determination of norepinephrine, uric acid and tyrosine. Mater Sci Eng B 226:132–140

[37] Kanchana P, Lavanya N, Sekar C (2014) Development of amperometric L-tyrosine sensor based on Fe-doped hydroxyapatite nanoparticles. Mater Sci Eng C 35:85–91
[38] Yang Z, Zhang C (2011) Molecularly imprinted hydroxyapatite thin film for bilirubin recognition. Biosens Bioelectron 29:167–171
[39] Yang Z et al (2014) Photoelectrochemical bilirubin biosensor based on Fe_3O_4/hydroxyapatite/molecularly imprinted polypyrrole nanoparticles. Sens Actuators B Chem 201:167–172
[40] Shahamirifard SA, Ghaedi M (2019) A new electrochemical sensor for simultaneous determination of arbutin and vitamin C based on hydroxyapatite-ZnO-Pd nanoparticles modified carbon paste electrode. Biosens Bioelectron 141:111474
[41] Erdem A, Congur G (2018) Hydroxyapatite nanoparticles modified graphite electrodes for electrochemical DNA detection. Electroanalysis 30:67–74
[42] Hend S et al (2021) Electrochemical impedance spectroscopy (EIS): principles, construction, and biosensing applications. Sensors 21:6578
[43] Cho H et al (2022) Electrochemical impedance-based biosensors for the label-free detection of the nucleocapsid protein from SARS-CoV-2. ACS Sens 7:1676–1684
[44] Chawla K et al (2018) Impedance-based microfluidic assay for automated antischistosomal drug screening. ACS Sens 3:2613–2620
[45] Meng T et al (2020) Construction of an ultrasensitive electrochemical sensing platform for microRNA-21 based on interface impedance spectroscopy. J Colloid Inter Sci 578:164–170
[46] Teengam P et al (2018) Electrochemical impedance-based DNA sensor using pyrrolidinyl peptide nucleic acids for tuberculosis detection. Anal Chim Acta 1044:102–109
[47] El-Sheikh SM et al (2021) A novel Ag/Zn bimetallic MOF as a superior sensitive biosensing platform for HCV-RNA electrochemical detection. App Surf Sci 562:150202
[48] Miller JN, Miller JC (2005) Statistics and chemometrics for analytical chemistry. Pearson Education, London, p 121–125
[49] Pang SN et al (2022) Urinary microRNA sensing using electrochemical biosensor to evaluate colorectal cancer progression. Biomedicines 10:1434
[50] Ouyang R et al (2023) Ti_3C_2@Bi_2O_3 nanoaccordion for electrochemical determination of miRNA-21. Microchim Acta 190:52
[51] Chai H et al (2021) Ultrasensitive electrochemical detection of miRNA coupling tetrahedral DNA modified gold nanoparticles tags and catalyzed hairpin assembly. Anal Chim Acta 1165:338543
[52] Liu S et al (2023) A novel detection of MicroRNA based on homogeneous electrochemical sensor with enzyme-assisted signal amplification. Talanta 256:124263
[53] Wang Q et al (2021) Ultrasensitive electrochemical detection of miRNA based on polymerization signal amplification. Talanta 235:122744
[54] Zhang Q, Guo Z, Zheng X (2023) Synthesis of Ag@carbonized polymer dots and their electrochemical sensing of miRNA. Electroanalysis 35:2200190
[55] Zheng Y et al (2021) Dual-mode biosensor for femtomolar miRNA-155 detection by electrochemiluminescence and adsorptive stripping voltammetry. Microchem J 165:106091
[56] Hu M et al (2021) CoNi bimetallic metal–organic framework as an efficient biosensing platform for miRNA 126 detection. App Surf Sci 542:148586
[57] Vural OA et al (2021) Human serum albumin–gold nanoparticle based impedimetric sensor for sensitive detection of miRNA-200c. Electroanalysis 33:925–935
[58] Li D et al (2019) Exosomes from miR-21-5p-increased neurons play a role in neuroprotection by suppressing rab11a-mediated neuronal autophagy in vitro after traumatic brain injury. Med Sci Monit 25:1871–1885
[59] Chen Z et al (2023) Specific adsorption of magnetic Fe_3O_4@hydroxyapatite nanocomposites to a hybridized duplex for immobilization and label-free electrochemical biosensing of microRNA. ACS Appl Nano Mater 6(10):8584–8592
[60] Kuang Y et al (2019) Duplex-specific nuclease-mediated amplification strategy for mass spectrometry quantification of miRNA-200c in breast cancer stem cells. Anal Chem 91:8820–8826